Bull Eng Geol Environ (2019) 78:857–866
DOI 10.1007/s10064-017-1150-0

ORIGINAL PAPER

Estimating the three-dimensional joint roughness coefficient value of rock fractures

Ping Mo[1] · **Yanrong Li**[1]

Received: 28 March 2017 / Accepted: 20 August 2017 / Published online: 8 September 2017

Abstract Measurement and estimation of the joint roughness coefficient (JRC) is a critical but also difficult challenge in the field of rock mechanics. Parameters for estimating JRC based on a profile derived from a fracture surface are generally two-dimensional (2D), where a single or multiple straight profiles derived from a surface cannot reflect the roughness of the entire surface. It is therefore necessary to derive the three-dimensional (3D) roughness parameters from the entire surface. In this article, a detailed review is made on 3D roughness parameters along with classification and discussion of their usability and limitations. Methods using Triangulated Irregular Network (TIN) and 3D wireframe to derive 3D roughness parameters are described. Thirty-eight sets of fresh rock blocks with fractures in the middle were prepared and tested in direct shear. Based on these, empirical equations for JRC estimation using 3D roughness parameters have been derived. Nine parameters (θ_s, θ_g, θ_{2s}, S_{sT}, S_{sF}, V_{an}, Z_{sa}, Z_{rms}, and Z_{range}) are found to have close correlations with JRC and are capable of estimating JRC of rock fracture surfaces. Other parameters (Z_{ss}, Z_{sk}, V_{svi}, V_{sci}, S_{dr} and S_{ts}) show no good correlations with JRC. The sampling interval has little influence when using volume and amplitude parameters (V_{an}, Z_{sa}, Z_{rms}, and Z_{range}) for JRC estimation, while it influences to some extent when other parameters (θ_s, θ_g, θ_{2s}, S_{sT} and S_{sF}) are used. For their easy calculation, the equations with amplitude parameters are recommended to facilitate rapid estimation of JRC in engineering practice.

✉ Yanrong Li
li.dennis@hotmail.com

[1] Taiyuan University of Technology, Taiyuan 030024, China

Keywords JRC estimation · Empirical equation · 3D roughness parameter · Sampling interval

Introduction

The rock joint roughness coefficient (JRC) was proposed by Barton (1973) to estimate the peak shear strength of joints using the following empirical equation, which is also called the JRC-JCS model:

$$\tau = \sigma tan\ [JRClog\ (JCS/\sigma) + \varphi_b] \quad (1)$$

where τ is the peak shear strength of the rock joint, σ is the normal stress, JRC is the joint roughness coefficient, JCS is the strength of joint wall, and φ_b is the basic friction angle.

Measurement and estimation of the JRC is critical for using the JRC-JCS model but also a difficult challenge in the field of rock mechanics (Barton and Bandis 1990). The JRC of a particular rock joint profile is most often estimated by visibly comparing it to the ten standard profiles with JRC values ranging from 0 to 20 (Barton and Choubey 1977). This approach has also been adopted by the ISRM (International Society for Rock Mechanics) Commission on Testing Methods since 1981 (Brown, 1981). However, the visible comparison is subjective since the user has to judge which profile the joint in question fits the best.

The development of objective methods was gradually advanced by researchers considering statistical parameters and the fractal dimension of the rock joint profiles. The most often used parameters include Z_2 (the root mean square of the first deviation of the profile), σ_I (standard deviation of the angle I), R_z (the maximum height), λ (the ultimate slope), δ (profile

elongation index), λ_{Z2} (directional roughness index), $\beta_{100\%}$ (average slope angle against shear direction), D_c (fractal dimension determined by compass-walking method), and D_{h-L} (fractal dimension determined via hypotenuse leg method). Among these, amplitude parameters (R_z, λ and D_{h-L}) show a lower sensitivity to the sampling interval (SI) than slope (Z_2, $\beta_{100\%}$, and σ_1) and elongation parameters (δ) in the determination of two-dimensional (2D) JRC (Li et al. 2016; Zheng and Qi 2016; Liu et al. 2017). Correlations between these parameters and JRC can be found in Tse and Cruden (1979), Yu and Vayssade (1991), Wakabayashi and Fukushige (1992), Tatone and Grasselli (2010), and Zhang et al. (2014), and in the reviews by Li and Zhang (2015), Li and Huang (2015), and Zheng and Qi (2016). However, these correlations are all based on 2D roughness profiles, i.e., cross-sections along straight lines over the joint surface. There are no well-developed methods to achieve roughness parameters for the entire fracture surface and no reliable equations for estimating JRC with such parameters.

This study gives a detailed review on parameters describing the roughness of an entire surface along with a classification and discussion about their usability and limitations. Methods using Triangulated Irregular Network (TIN) and three-dimensional (3D) wireframe to derive 3D roughness parameters are proposed. Based on direct shear tests of 38 sets of rock joints, a set of empirical equations are proposed for JRC estimation using 3D roughness parameters.

Literature review

A detailed literature review of 3D roughness parameters representing an entire fracture surface is summarized in this section. Most morphological reconstructions of fracture surfaces are realized by the 3D wireframe (curved rectangle) model (Belem et al. 2000; Zhang et al. 2009) or TIN model (Belem et al. 2000; Grasselli 2001; Cottrell 2009; Grasselli and Egger 2003; Lee et al. 2011; Tang et al. 2012). Elements of the 3D wireframe or TIN have their own physical properties including dip angle, dip direction, height, area, etc. Parameters with the same physical significance proposed by different researchers can be classified into four groups of slope, area, volume, and amplitude.

Slope parameters are related to dip angle or apparent dip angle of the elements of 3D wireframe or TIN models. Grasselli (2001) rebuilt the fracture surface by TIN and took apparent dip angle (θ^*) of the elements against shearing direction and potential area ratio ($A_{\theta*}$) of TIN elements to describe the roughness of fracture surface. The area ratio is given by $A_{\theta*} = A_{pi} / A_t$, where A_{pi} is the total area of triangular elements against the shear direction with apparent slopes larger than θ^* and A_t is the actual area of the

Table 1 Three-dimensional slope parameters describing fracture surface roughness

Term	Definition	Calculation	Original	Anisotropy	E^{JRC}	References
θ_{ci}	Slope index of element surfaces facing shearing direction	$\theta_c = \theta^*_{max}/(1 + C)$	θ^*_{max}/C; $\theta^*_{max}/(1 + C)$	√	√	Grasselli (2001); Cottrell (2009); Grasselli and Egger (2003); Tatone and Grasseli (2010)
θ_s	Surface angularity of the entire surface	$\theta_s = \frac{1}{n}\sum_{i=1}^{n}\alpha_{ij}$	θ_s		√	Belem et al. (2000); Lee et al. (2011); Tang et al. 2012)
θ_{si}	Surface angularity of element surfaces facing shearing direction	$\theta_{si} = \frac{1}{m_s}\sum_{i=1}^{m_s}\alpha_{ij,s}$	θ_s'	√	√	Lee et al. (2011)
θ_{2s}	Root mean square of the slopes of entire surface	$\theta_{2s} = \sqrt{\frac{\sum\sum tan^2\alpha_{ij}}{n}}$	Z_{2s}; S_{dq}; Z_2			Belem et al. (2000); Zhang et al. (2009)
θ_{2si}	Root mean square of the slopes facing shearing direction	$\theta_{2si} = \sqrt{\frac{\sum\sum tan^2\alpha_{ij,s}}{m_s}}$	$Z_{2,k}$	√	√	Zhang et al. (2009)

α_{ij} actual dip angle of the elements of 3D wireframe, $\alpha_{ij,s}$ actual dip angle of elements facing shearing direction of 3D wireframe, θ^*_{max} maximum apparent angle of the triangular elements in shearing direction, 3D three-dimensional, Anisotropy parameters allowing consideration of shear direction, C a fitted value, E^{JRC} parameters used in published empirical equations, m_s total number of the elements facing shearing direction of 3D wireframe, n total number of the elements of 3D wireframe

Table 2 Three-dimensional area parameters describing fracture surface roughness

Term	Definition	Calculation	Original	Anisotropy	E^{JRC}	References
S_s	Ratio of actual and nominal areas	$S_s = \frac{A_t}{A_n}$	R_s; R_s–1; S_{ts}; SR_s; S_{dr}			El-Soudani (1978); Belem et al. (2000); Belem et al. (2009)
S_{bap}	Brightened area percentage	$S_{bap} = \frac{A_b}{A_t} \times 100\%$	BAP	√	√	Ge et al. (2012)
S_{dr}	Degree of joint interface relative surface roughness	$S_{dr} = 1–1/S_s$	DR_r			Belem et al. (2000)
S_{ts}	Surface tortuosity coefficient	$S_{ts} = \frac{A_t}{A_n} cos\phi$	T_s			Belem et al. (2000)

A_t actual area, A_b: brightened area of fracture surface under a simulated parallel light, A_n nominal area, cosϕ tortuosity index of the least square plane of the four extreme marginal points of the surface

surface. Based on this, Grasselli (2001) proposed a 3D parameter θ^*_{max}/C:

$$A_{\theta^*} = A_0 \left(\frac{\theta^*_{max} - \theta^*}{\theta^*_{max}} \right)^C \tag{2}$$

where θ^*_{max} is the maximum apparent dip angle of the elements against shearing direction, C is a fitted value calculated via non-linear least-squares regression, and A_0 is the value of $A_{\theta*}$ when θ^* equals 0. However, Cottrell (2009) argued that parameter suggested by Grasselli (2001) has no physical meaning when C equals 0 and revised it by proposing parameter $\theta^*_{max}/(1 + C)$, which is accepted by Tatone and Grasselli (2010). $\theta^*_{max}/(1 + C)$ is abbreviated as θ_{ci} for later use in the present study.

Belem et al. (2000) proposed the mean (θ_s) and the root mean square (θ_{2s}) of the actual dip angle of the elements for an entire surface to describe surface roughness. Lee et al. (2011) updated θ_s as proposed by Belem et al. (2000) to θ_{si} by adopting the elements facing the shear direction. Zhang et al. (2009) revised θ_{2s} as proposed by Belem et al.(2000) into θ_{2si} by adopting only the elements facing the shear direction. Definitions and calculations of the slope parameters are shown in Table 1.

Parameters related to area include actual area, nominal area, shearing area, etc. of the elements or entire surface. The ratio (S_s) between the actual area and the nominal area was first defined as a surface roughness index by El-Soudani (1978). S_s was revised by Belem et al. (2000) for both upper and lower fracture surfaces. Grasselli (2001) stated that it is correct

Table 3 Three-dimensional volume and amplitude parameters describing fracture surface roughness

Term	Definition	Parameter	Original	References
Z_{rms}	Root mean square height of z	$Z_{rms} = \left(\frac{1}{N} \iint z_{ij}^2 dxdy \right)^{1/2}$	RMS; S_q	Marlinverno (1990) Fan et al. (2013)
Z_{Sz}	Ten-point height	$Z_{Sz} = \frac{\sum_1^5 \lvert z_{pi} \rvert + \sum_1^5 \lvert z_{vi} \rvert}{10}$	S_z	ISO 25178–2: 2012
Z_{sa}	Mean of the absolute of z	$Z_{sa} = \frac{1}{m \times n} \sum_{j=1}^{m} \sum_{I=1}^{n} \lvert z_{ij} \rvert$	S_a	ISO 25178–2: 2012 Fan et al. (2013)
Z_{ss}	Skewness of the surface	$Z_{ss} = \frac{\frac{1}{m \times n} \sum_{j=1}^{m} \sum_{I=1}^{n} z_{ij}^3}{Z_{rms}^3}$	S_{sk}	ISO 25178–2: 2012
Z_{sk}	Kurtosis of the surface	$Z_{sk} = \frac{\frac{1}{m \times n} \sum_{j=1}^{m} \sum_{I=1}^{n} z_{ij}^4}{Z_{rms}^4}$	S_{kw}	ISO 25178–2: 2012
Z_{range}	Range of z	$Z_{range} = z_{max} - z_{min}$	$Range$; S_p	ISO 25178–2: 2012 Fan et al. (2013)
V_{svi}	Valley fluid retention index	$V_{svi} = \frac{V_v(h_{0.8})}{Z_{rms}(M-1)(N-1)\Delta x \Delta y}$	S_{vi}	ISO 25178–2: 2012
V_{sci}	Core fluid retention index	$V_{sci} = \frac{V_v(h_{0.05}) - V_v(h_{0.8})}{Z_{rms}(M-1)(N-1)\Delta x \Delta y}$	S_{ci}	ISO 25178–2: 2012

$V_v(h_{0.8})$ void volume at the surface heights at 80% bearing area, $V_v(h_{0.05})$ void volume at the surface heights at 5% bearing area, Z_{ij} heights of point cloud of scanned surface, z_{pi} five highest peaks of point cloud of scanned surface (i = 1, 2, …, 5), z_{vi} five lowest troughs of point cloud of scanned surface, Z_{max} highest peaks of point cloud of scanned surface, Z_{min} lowest troughs of point cloud of scanned surface

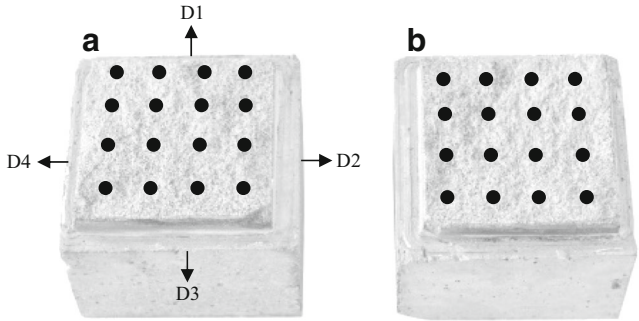

Fig. 1 Tested rock joint samples: (a) lower fracture surface; and (b) upper fracture surface. The dots show the pattern of points tested for strength of the joint wall (JCS). D1–D4 indicate the four succeeding shearing directions in direct shear tests on each specimen

to assume that the upper and lower fracture surfaces of fresh joint are in 100% contact for JRC estimation.

Ge et al. (2012) proposed S_{bap}, the percentage of the bright area over the actual fracture surface area, as a 3D roughness parameter. However, they did not specify an optimum incident angle for the parallel light for the estimation of JRC. Belem (2000) proposed similar 3D roughness parameters, S_{dr} and S_{ts}, which are also based on A_t and A_n (nominal area). Details of area parameters are listed in Table 2.

Most parameters related to amplitude or volume of the surface elements are cited by geometrical specifications (ISO 25178–2: 2012). There are six parameters (Z_{rms}, Z_{sz}, Z_{sa}, Z_{ss}, Z_{sk}, and Z_{range}) related to amplitude and two parameters (V_{svi} and V_{sci}) related to volume. Definitions and calculations of these parameters are given in Table 3.

Although many 3D parameters were suggested for quantifying surface roughness, only a few slope and area parameters were examined in developing empirical equations predicting JRC (θ_{ci}, θ_s, θ_{si}, θ_{2si}, and S_{bap} in Tables 1 and 2). Grasselli's (2001) experiments and corresponding roughness parameters (θ_{ci}) have no direct relationship with the JRC of rock fracture surfaces. Empirical equations proposed by Tatone (2009), which are linked to JRC, are only based on the ten 2D standard profiles by Barton (1976). Zhang et al. (2009) used the 3D parameter θ_{2si} in a 2D empirical equation by Tse and Cruden (1979). Ge et al. (2012) derived an empirical equation for an unknown incident angle of the parallel light. In addition, few 3D empirical equations take SIs into consideration. Lee et al. (2011) made a comparison of JRC with surface angularity θ_s at SIs of 0.2, 0.3, 0.5, 1.0, 2.0, and 5.0 mm but suggested empirical equations with a fixed optimum sampling interval. However, it has been stated by Yang et al. (2001), Li et al. (2016), Zheng and Qi (2016), and Liu et al. (2017) that sampling intervals might shift the relationship between the JRC and roughness parameters.

Considering the restrictions and limited scope of the above-mentioned findings, a set of reliable 3D roughness parameters and correlations between such parameters and JRC are required. This objective can be successfully achieved via direct shear tests on a large sample population and success in achieving 3D roughness parameters.

Table 4 Mechanical properties of the fracture surfaces

Sample no.	φ_b (°)	JCS (MPa)	σ_n/JCS	τ (kPa)	STD
1	28.0	33.62	0.01	585.38	60.1
2	30.6	25.93	0.02	672.42	35.2
3	28.0	15.02	0.03	710.05	135.0
4	28.0	28.69	0.02	670.76	83.5
5	28.0	26.41	0.02	458.71	48.3
6	28.0	31.94	0.02	629.93	160.2
7	28.0	21.95	0.02	617.60	91.1
8	28.0	20.13	0.02	619.29	143.8
9	28.0	18.30	0.03	356.84	93.3
10	28.0	28.95	0.02	607.11	47.0
11	29.7	36.06	0.01	352.57	16.7
12	28.0	23.08	0.02	703.71	66.0
13	24.1	71.19	0.01	223.50	8.9
14	27.9	39.29	0.01	530.50	128.5
15	27.9	42.99	0.01	697.75	50.0
16	27.9	41.50	0.01	659.50	97.7
17	27.9	37.49	0.01	627.00	66.5
18	27.9	36.27	0.01	717.75	125.5
19	27.9	40.94	0.01	641.50	93.0
20	27.9	33.71	0.01	820.75	61.2
21	27.9	40.71	0.01	668.50	73.8
22	27.8	53.76	0.01	852.79	65.8
23	27.9	27.37	0.02	248.50	61.2
24	27.9	25.47	0.02	453.25	91.4
25	27.9	71.01	0.01	264.75	4.8
26	27.8	47.47	0.01	491.19	80.7
27	27.9	31.85	0.02	695.75	73.4
28	27.8	42.75	0.01	460.87	47.8
29	27.8	51.81	0.01	537.75	58.2
30	27.8	35.76	0.01	706.17	72.8
31	27.8	47.09	0.01	518.86	47.4
32	27.8	67.60	0.01	406.13	73.3
33	27.8	67.60	0.01	409.09	26.3
34	27.8	51.81	0.01	480.37	97.9
35	27.8	63.20	0.01	473.90	66.5
36	27.8	56.50	0.01	417.60	77.3
37	27.8	55.62	0.01	448.68	39.6
38	27.9	44.76	0.01	645.50	98.8

JCS strength of the joint wall, STD standard deviation of measured peak shear strengths

Experiments

Mechanical properties and surface geometry of rock joints are the two key parts of this study. Sample preparations,

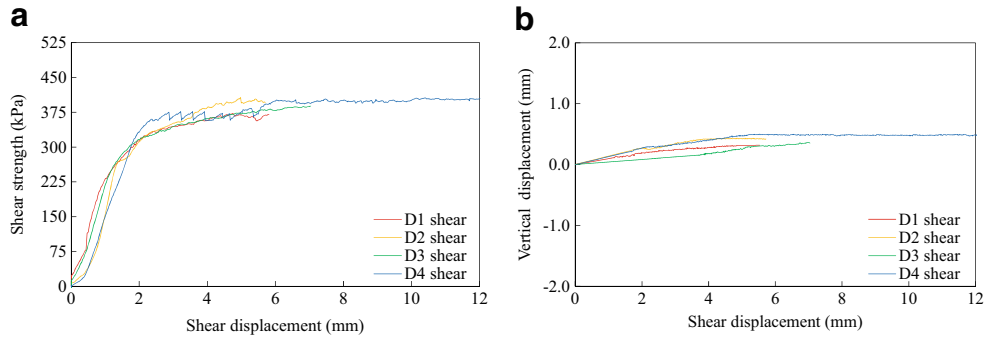

Fig. 2 Representative plots of direct shear tests: (a) shear stress vs. shear displacement; and (b) vertical displacement vs. shear displacement. D1–D4 indicate the four succeeding shearing directions in direct shear tests on each specimen

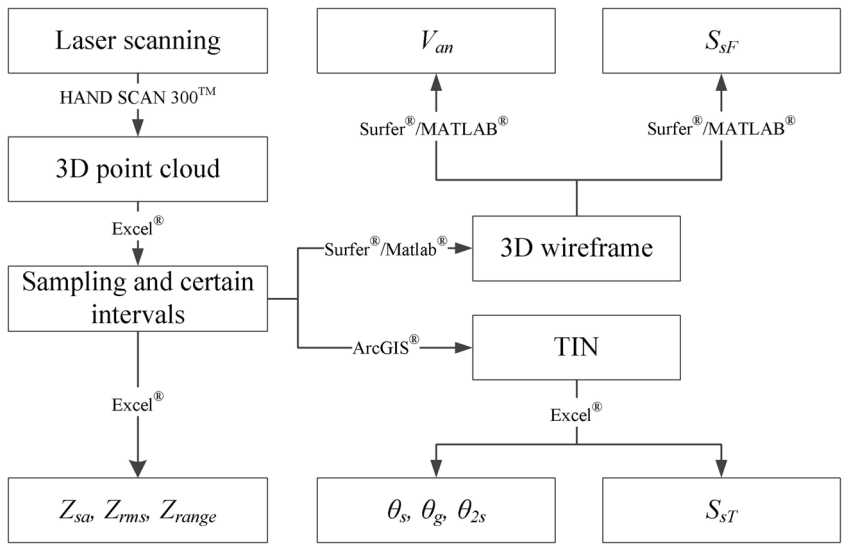

Fig. 3 Flowchart for determining the three-dimensional roughness parameters of a rock joint. 3D three-dimensional, TIN Triangulated Irregular Network

mechanical tests, and surface measurements to describe these components are summarized in the following sections.

Sample preparation

We collected 38 groups of fresh rock blocks with structural planes in the middle, of which nine were limestone, 12 granite, and 17 sandstone. The structural planes of these samples have varied roughness, from smooth to extremely rough, forming a sequence. Samples of limestone and sandstone were collected from rock cores. The rest were artificially produced by splitting granite blocks. The upper and lower fracture surfaces of all specimens were fresh and matched well, showing no obvious aperture and infilling. The length and width of the rock specimens were restricted to 120 mm × 120 mm and each specimen was cemented into a 150 mm × 150 mm × 223.5 mm concrete block. Great attention was paid to aligning the joint surfaces of the concreted specimens so that they were as horizontal as possible (Fig. 1). This was done by putting reference lines, which were parallel to the main inclination of the joint surface, along the periphery of the specimens and rotating the specimens to make the reference lines aligned horizontally during sample preparation.

Mechanical properties

According to Barton's JRC-JCS model, the JRC of rock fracture can be back-calculated if the strength of peak shear strength (τ), joint wall (JCS), and basic friction angle (φ_b) of the fracture were known.

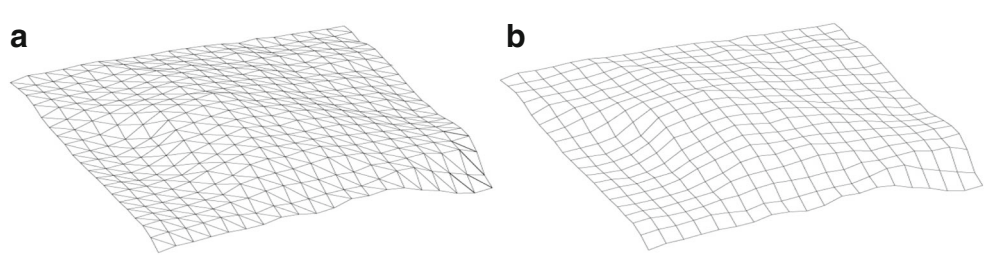

Fig. 4 The morphological reconstruction of the fracture surface: (a) Triangulated Irregular Network (TIN); and (b) three-dimensional wireframe

Peak shear strength of the 38 prepared joint specimens were measured using the direct shear test. The normal stress was set to 500 kPa, corresponding a depth of 15–25 m, to simulate the actual in situ conditions of the samples. The shear rate was 0.3 mm/min for all specimens. Each specimen's four sides are marked as D1–D4 and sheared in these directions successively (Fig. 1). The average value and standard deviation of measured peak shear strengths (D1–D4) of each specimen are given in Table 4. Representative curves of shear stress and vertical displacement versus shear displacement are shown in Fig. 2. The curves of shear stress versus shear displacement follow the similar pattern for all four directions.

In the determination of the rebound value, 32 points on each specimen are tested using a Schmidt rebound hammer (Fig. 1). The rebound value for each surface is calculated from the average. The JCS of the specimen is then calculated according to Aydin (2009). The basic-friction angle (φ_b) is measured using tilt tests on saw-cut dry joint surfaces. The mechanical properties of the fracture surfaces are listed in Table 4.

Surface measurements

With the help of laser scanning technology (HAND SCAN™ 300, resolution of 0.1 mm and accuracy of 0.04 mm), the morphology of each fracture surface can be digitized into a point cloud. In this study, both upper and lower fracture surfaces of the 38 sets of samples were scanned before and after shearing with 0.2 mm spatial resolution. Fig. 3 shows the steps to derive roughness parameters of joint surfaces. Grid data sets were constructed by sampling the point cloud at different intervals (0.4, 0.8, 1.6, 3.2, and 6.4 mm) using Microsoft Excel®. The grid data sets were then used to build TIN and 3D wireframe models (Fig. 4) using ArcGIS®, Surfer®, and MATLAB® programs. The amplitude parameters (e.g., Z_{sa}, Z_{rms} and Z_{range}) were derived directly from the 3D point cloud through Excel® calculation, slope parameters (θ_s and θ_{2s}) were derived from TIN models, volume parameters (V_{an}) were derived from 3D wireframe models, and area parameters (S_{sT} and S_{sF}) were derived from TIN and 3D wireframe models using Excel® .

The variations (V) of amplitude parameters (Z_{rms}, Z_{sa}, Z_{range}) between upper and lower surfaces (e.g., V_{rms} = the ratio of [Z_{rms} of upper surface – Z_{rms} of lower surface] to Z_{rms} of lower surface) were examined and are shown in Table 5. It was found that the maximum variation is about − 4.68%, indicating that both sides of the joints match well. Grasselli (2001) and Belem et al. (2000) demonstrated that fresh joints have few voids in between both sides. Fan et al. (2013) also indicated that the S_s and θ_{2s} values of each set of coupled joints are quite close.

The first three shear tests (D1, D2, and D3) ceased at a shear displacement of about 6 mm to capture the peak strength. The last shearing (D4) was stopped at a shear displacement of more than 30 mm. This strategy was originally designed to gain the residual strength of the joint from the last test. The difference of amplitude parameters between pre- and post-shear fracture surfaces is less than 2.16% (Table 5), indicating there is no obvious damage induced by shearing. This is

Table 5 Variation of height parameters between upper and lower joint surfaces and difference of height parameters between pre- and post-shear surfaces

Sample no.	Variation of height parameters between upper and lower surface (%)			Difference of height parameters between pre- and post-shear surfaces (%)		
	V_{rms}	V_{sa}	V_{range}	D_{rms}	D_{sa}	D_{range}
1	− 2.78	− 3.18	− 3.49	0.30	0.29	0.44
2	1.41	1.48	1.49	0.08	0.09	0.13
3	− 2.43	−2.61	− 2.70	0.29	0.30	0.4
4	1.28	1.44	1.50	0.90	0.90	1.35
5	2.89	2.99	3.10	0.41	0.42	0.42
6	− 0.91	− 1.02	− 1.08	1.14	1.17	1.18
7	2.73	3.15	3.20	0.04	0.05	0.05
8	2.84	3.20	3.51	0.24	0.25	0.25
9	− 3.07	− 3.52	− 3.83	0.37	0.37	0.56
10	− 3.19	− 3.72	− 3.76	1.24	1.27	1.28
11	1.63	1.76	1.76	1.10	1.12	1.13
12	2.50	2.75	2.90	0.19	0.19	0.28
13	2.47	2.76	2.78	0.71	0.72	1.08
14	− 4.68	− 4.68	− 2.93	0.14	0.14	0.23
15	1.37	1.37	1.62	0.06	0.06	0.26
16	− 3.02	− 3.01	0.83	0.06	0.06	1.49
17	− 2.25	− 2.25	− 0.49	0.10	0.11	1.43
18	0.56	0.59	0.30	0.32	0.32	1.52
19	2.54	2.60	2.62	0.60	0.60	0.10
20	1.19	1.32	1.45	0.76	0.76	1.44
21	− 0.18	− 0.20	− 0.21	0.24	0.24	0.61
22	2.34	2.81	3.04	0.29	0.29	0.44
23	1.84	2.03	2.09	1.09	1.07	1.60
24	0.96	1.05	1.10	0.87	0.89	0.90
25	0.48	0.56	0.59	1.07	0.64	1.34
26	2.40	2.79	2.89	0.66	0.65	1.23
27	− 2.12	− 2.33	− 2.33	0.47	0.48	2.16
28	2.99	3.38	3.65	1.04	1.06	2.02
29	− 1.60	− 1.78	− 1.93	0.89	0.87	1.31
30	− 2.51	− 2.77	− 2.87	1.15	1.17	1.18
31	1.65	1.87	2.03	0.09	0.09	0.09
32	2.34	2.51	2.73	1.14	1.17	1.18
33	2.77	3.02	3.05	0.66	0.66	0.67
34	0.77	0.86	0.93	0.52	0.53	0.54
35	− 3.13	− 3.39	− 3.55	0.12	0.13	0.13
36	2.82	2.89	3.06	1.00	1.02	1.03
37	0.73	0.81	0.84	0.45	0.46	0.47
38	− 1.57	− 1.79	− 1.81	0.28	0.27	0.36

D_{range} difference of Z_{range} ($D_{range} = \frac{Z_{range}{}^{post} - Z_{range}{}^{pre}}{Z_{range}{}^{pre}}$), D_{rms} difference of Z_{rms} ($D_{rms} = \frac{Z_{rms}{}^{post} - Z_{rms}{}^{pre}}{Z_{rms}{}^{pre}}$), D_{sa} difference of Z_{sa} ($D_{sa} = \frac{Z_{sa}{}^{post} - Z_{sa}{}^{pre}}{Z_{sa}{}^{pre}}$), V_{range} variation of Z_{range} ($V_{range} = \frac{Z_{range}{}^{upper} - Z_{range}{}^{lower}}{Z_{range}{}^{lower}}$), V_{rms} variation of Z_{rms} ($V_{rms} = \frac{Z_{rms}{}^{upper} - Z_{rms}{}^{lower}}{Z_{rms}{}^{lower}}$), V_{sa} variation of Z_{sa} ($V_{sa} = \frac{Z_{sa}{}^{upper} - Z_{sa}{}^{lower}}{Z_{sa}{}^{lower}}$); the superscript "upper" and "lower" stand for the parameter derived from the upper or lower joint surface, respectively; the superscript "post" indicates that the parameter is derived from joint surface after the 4th shearing, while "pre" means that the parameter is derived from joint surface before the 1st shearing

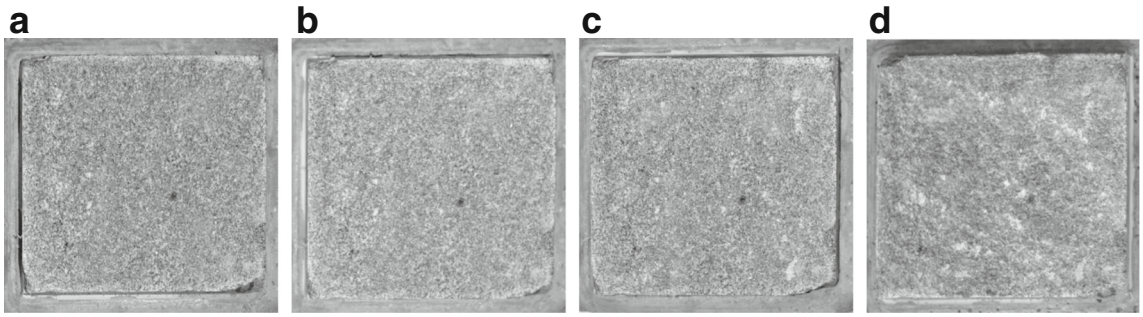

Fig. 5 Photos of fracture surface of sample 1 sheared in different directions of: (a) D1; (b) D2; (c) D3; and (d) D4. D1–D4 indicate the four succeeding shearing directions in direct shear tests on each specimen

evident in the photos of post-shear joint surfaces (Fig. 5). The stress level (500 kPa/JCS) is less than 0.03 for all tests (Table 4). This also protects the fracture surface from being damaged during shearing. Considering this, the lower surface was used to represent the coupled joint surfaces and its original morphology was used to generate the 3D roughness parameters for later calculation and analysis.

Empirical equations for the entire surface

Considering the anisotropy of rock joints and uncertainty of shear direction in real rock engineering, we propose use of average peak strength (average value from the four direction shears) for the back-calculation of JRC. Accordingly, the roughness parameters should be direction-independent and valid for the entire surface.

Slope parameters

As shown in Table 1, θ_s and θ_{2s} do not consider shear direction, whereas θ_{si}, θ_{2si}, and θ_{ci} do. Therefore, θ_s and θ_{2s} were chosen and calculated for deriving empirical equations with the back-calculated JRC. In calculation of θ_s and θ_{2s}, previous researchers suggested deriving α_{ij} (dip angle of elements of the entire surface) from the 3D wireframe model (Belem et al. 2000, Lee et al. 2011 and Zhang et al. 2009). However, not every element in the 3D wireframe model is a quadrangle with all four corners in the same plane. This makes calculating α_{ij} difficult and inaccurate, since a least-square plane has to be constructed to substitute the real element. We suggest use of the TIN model rather than the 3D wireframe model to calculate α_{ij} and then slope parameters to reduce the calculation-induced deviation.

On the other hand, as θ_{ci} is also a parameter considering shear direction, we propose an equivalent parameter θ_g (Eq. 3), which is the integral of A_α. A_α is the ratio of A_p to A_t, where A_p is the total area of triangular elements whose actual dip angle is larger than α and A_t is the actual area of the surface.

$$\theta_g = \int_0^{\alpha_{max}} A_\alpha d\alpha \quad (3)$$

where, α_{max} is the maximum actual dip angle of the triangular elements.

θ_g avoids using the fitted value C (for calculating θ_{ci}), and it is much easier to calculate. The newly derived JRC estimation equations as functions of θ_s, θ_{2s}, and θ_g are listed in Table 6 and plotted in Fig. 6.

Area parameters

According to the definition of S_s in Table 2, two parameters, S_{sF} and S_{sT}, were obtained for each fracture surface from the constructed 3D wireframe and TIN models, respectively. Both of them show close correlations with JRC as shown in Table 6 and Fig. 7.

S_{dr} and S_s have a similar physical meaning (Table 2). In this study, S_{dr} exhibits lower correlation coefficients when it is

Table 6 Empirical equations of selected joint roughness coefficient coupling roughness parameters with sampling interval as independent variables

Variable	Equation	R^2
θ_s	$JRC = 2.9\theta_s^{0.7} + SI^{0.809} - 5.6$	0.902
θ_g	$JRC = 3.9\theta_g^{0.6} + SI^{0.815} - 7.7$	0.900
θ_{2s}	$JRC = 36.5S_{2s}^{0.5} + SI^{0.845} - 7.8$	0.883
S_{sT}	$JRC = 47.7(S_{sT} - 1)^{0.3} + SI^{0.836} - 6.7$	0.889
S_{sF}	$JRC = 47.8(S_{sF} - 1)^{0.3} + SI^{0.837} - 6.7$	0.888
V_{an}	$JRC = 43.9V_{an}^{0.1} + SI^{0.087} - 34.4$	0.824
Z_{sa}	$JRC = 58.5Z_{sa}^{0.1} - SI^{0.071} - 48.9$	0.804
Z_{rms}	$JRC = 63.2Z_{rms}^{0.1} + SI^{0.090} - 54.7$	0.798
Z_{range}	$JRC = 15.5\,Z_{range}^{0.2} + SI^{0.166} - 15.8$	0.759

θ_g threshold angle ($\theta_g = \int_0^{\alpha_{max}} A_\alpha d\alpha$), A_α threshold ratio for the entire surface ($A_\alpha = A_p/A_n$), A_p total area of the triangular elements whose actual dip angles are larger than α, A_n nominal area, JRC joint roughness coefficient, S_{sF} ratio of actual and nominal area of the three-dimensional wireframe, SI sampling interval, S_{sT} ratio of actual and nominal area of the Triangulated Irregular Network (TIN) surface, V_{an} ratio of the net volume of fracture surface to the projected area ($V_{an} = V_n/A_n$), V_n the summation of positive and negative volumes of the surface segmented by the least-square plane

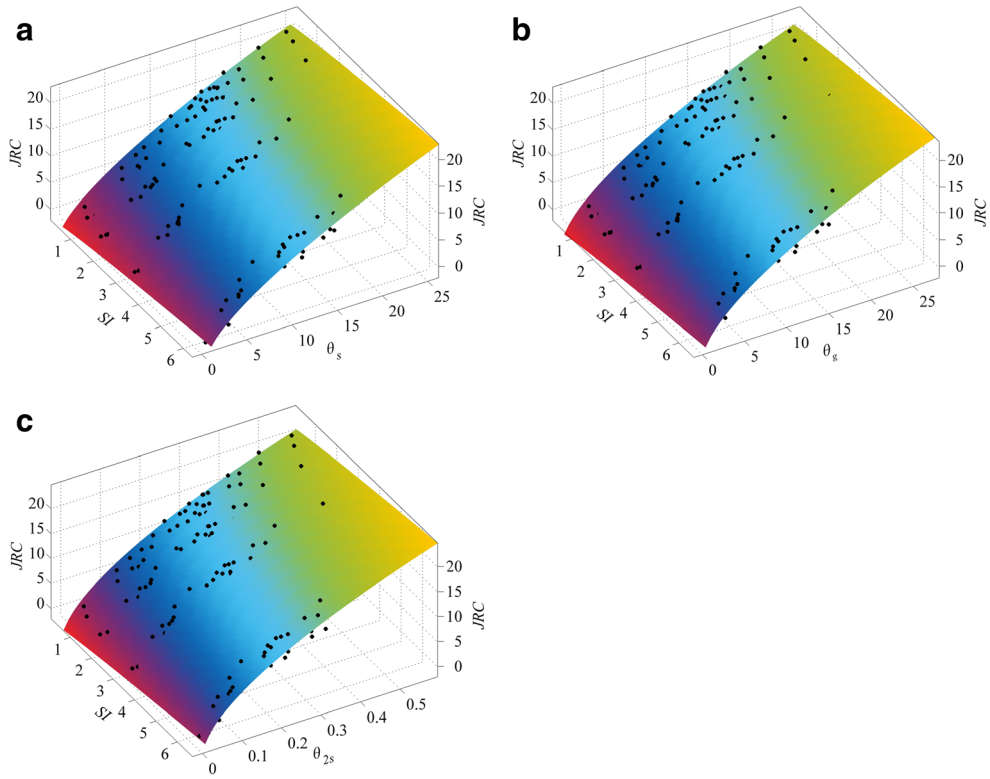

Fig. 6 Multiple regression of joint roughness coefficient (JRC), sampling interval (SI), and roughness parameters of (a) θ_s; (b) θ_g; and (c) θ_{2s}

used to get regression correlations with JRC than S_{sF} and S_{sT}. Regression analysis was also done for S_{ts}, which gives very low correlation coefficient. This may be due to insufficient consideration by taking only four corner points of the fracture surface to calculate the tortuosity index (cosϕ) of the entire surface. We therefore excluded using S_{dr} and S_{ts} for the estimation of JRC.

Volume and amplitude parameters

Amplitude parameters Z_{sa} and Z_{sz} are based on the same measurements and are closely related. In this study, Z_{sa}, Z_{rms}, Z_{ss}, Z_{sk}, and Z_{range} were used. In addition, V_{svi} and V_{sci} demonstrated no good correlation with JRC (the correlation coefficients are less than 0.4). We propose a parameter, V_{an}, which is the ratio of the net volume of fracture surface (V_n) to the projected area (A_n). The net volume (V_n) is the summation of positive and negative volumes of the surface segmented by the least-square plane (Fig. 8). It is found that V_{an} has close correlation with JRC. Table 6 lists the newly derived equations for volume and amplitude parameters, which are plotted in Fig. 9. The parameters Z_{sk} and Z_{ss} show no relation with JRC.

Discussion

In general, the nine proposed equations in Table 6 are all capable of estimating the JRC of rock fracture surfaces as they

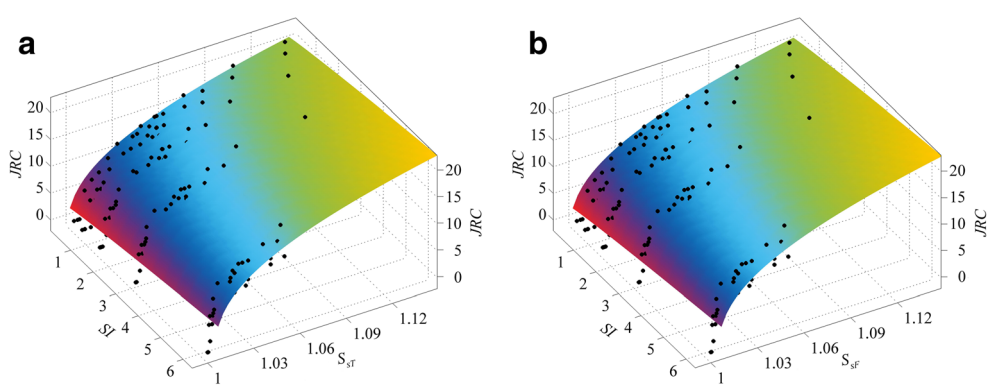

Fig. 7 Multiple regression of joint roughness coefficient (JRC), sampling interval (SI), and roughness parameters of (a) S_{sT}; and (b) S_{sF}

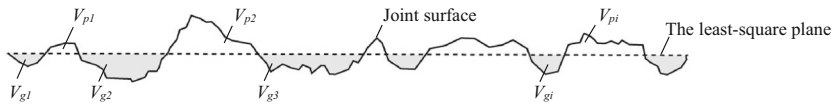

Fig. 8 Measurement of net volume (V_n) of the fracture surface

$V_n = \sum V_{pi} + \sum V_{gi}$, the net volume.
V_{pi}: the positive volume of the surface.
V_{gi}: the negative volume of the surface.

have correlation coefficients greater than 0.75. Among them, slope parameters perform the best and the amplitude parameters perform the worst in terms of correlation coefficient. Regarding the usability and applicability, the amplitude parameters (Z_{sa}, Z_{rms}, and Z_{range}) can be directly and easily calculated in Excel® once the point cloud is obtained by scanning the fracture surface. The calculation of V_{an} and S_{sF} is based on 3D wireframe and that of slope parameters (θ_s, θ_g, and θ_{2s}) and S_{sT} is based on the TIN model. They all require third-party software programs (e.g., Surfer®, MATLAB®, and ArcGIS® in this study) to deal with the point could. Considering the difficulties in a complex calculation for slope, area and volume parameters, one can chose the amplitude parameters to facilitate rapid estimation of JRC in engineering practice.

The regression correlations in Table 6 indicate that the sampling interval has some influence on the estimation of JRC, especially when slope and area parameters are used. Li et al. (2016) and Liu et al. (2017) also found that slope parameters (Z_2, $\beta_{100\%}$, and σ_i) show much higher sensitivity to the sampling interval than amplitude parameters (R_z, λ, and D_{h-L}) in the determination of 2D JRC. Although the sampling intervals used in this study (0.2–6.4 mm) cover a wide scope, great caution should be paid when employing the proposed equations for other sampling intervals.

The stress level (500 kPa/JCS) used in this study was designed for simulating the actual in situ conditions of the tested samples, which were collected from the depth of 15–25 m, and for protecting the fracture surface from being damaged during shearing. The proposed equations are suggested to be used for rock joints in shallow layers or for joints whose surfaces are hardly altered during shearing.

Conclusion

For decades, objective and quantitative determination of JRC were investigated mostly for the parameters derived from a 2D profile. However, a single or multiple straight-line profiles collected from a fracture surface cannot reflect the roughness of the entire surface. This study reviews roughness parameters

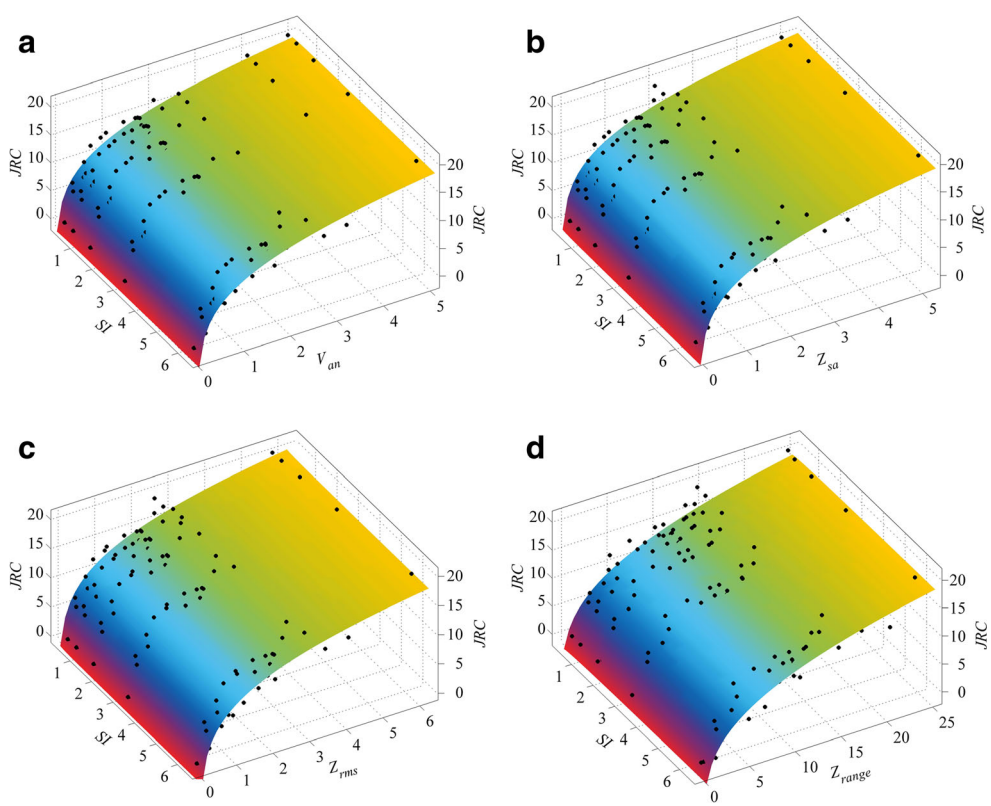

Fig. 9 Multiple regression of joint roughness coefficient (JRC), sampling interval (SI), and roughness parameters of (a) V_{an}; (b) Z_{sa}; (c) Z_{rms}; and (d) Z_{range}

derived from 3D surfaces and conducts relevant experiments. Back-calculated JRC values from 38 rock blocks with existing fractures are used to derive new empirical equations as a joint function of roughness parameter and sampling interval for JRC estimation.

The following main conclusions can be made:

(1) Nine parameters (θ_s, θ_g, θ_{2s}, S_{sT}, S_{sF}, V_{an}, Z_{sa}, Z_{rms}, and Z_{range}) are found to have close correlations with JRC and are capable of estimating the JRC of rock fracture surfaces. Other parameters (Z_{ss}, Z_{sk}, V_{svi}, V_{sci}, S_{dr}, and S_{ts}) show no good correlations with JRC.
(2) Slope parameters perform the best and the amplitude parameters perform the worst in terms of correlation coefficient.
(3) The sampling interval has little influence when using volume and amplitude parameters (V_{an}, Z_{sa}, Z_{rms}, and Z_{range}), while it influences to some extent when other parameters (θ_s, θ_g, θ_{2s}, S_{sT}, and S_{sF}) are used.

Acknowledgements This study was supported by the National Natural Science Foundation of China (No. 51309176).

References

Aydin A (2009) Suggested method for determination of the Schmidt hammer rebound hardness: revised version. Int J Rock Mech Min Sci 46(3):627–634

Barton N (1973) Review of a new shear-strength criterion for rock joints. Eng Geol 7:287–332

Barton N (1976) The shear strength of rock and rock joints. Int J Rock Mech Min Sci Geomech Abstr 13(9):255–279

Barton N, Bandis S (1990) Review of predictive capabilities of JRC-JCS model in engineering practice. Proc Int Symp Rock Joints 182:603–610

Barton N, Choubey V (1977) The shear strength of rock joints in theory and practice. Rock Mech Rock Eng 10(1):1–54

Belem T, Homand-Etienne F, Souley M (2000) Quantitative parameters for rock joint surface roughness. Rock Mech Rock Eng 33(4):217–242

Belem T, Souley M, Homand F (2009) Method for quantification of wear of sheared joint walls based on surface morphology. Rock Mech Rock Eng 42(6):883–910

Brown ET (1981) Rock characterization testing and monitoring (ISRM suggested methods). Pergramon, Oxford

Cottrell B (2009) Updates to the GG-Shear Strength Criterion. M.Eng. thesis. University of Toronto at Toronto

El-Soudani SM (1978) Profilometric analysis of fractures. Metallography 11(3):247–336

Fan X, Cao P, Huang XJ, Chen Y (2013) Morphological parameters of both surfaces of coupled joint. J Cent South Univ 20(3):776–785

Ge YF, Tang MH, Huang L, Wang QL, Sun MJ, Fan YJ (2012) A new representation method for three-dimensional joint roughness coefficient of rock mass discontinuities. Chin J Rock Mech Eng 31(12):2508–2517

Grasselli G (2001) Shear strength of rock joints based on quantified surface description. Ph.D. thesis. Ecole Polytechnique Federale De Lausanne (EPFL)

Grasselli G, Egger P (2003) Constitutive law for the shear strength of rock joints based on three-dimensional surface parameters. Int J Rock Mech Min Sci 40(1):25–40

ISO 25178-2 (2012) Geometrical Product Specifications (GPS) – Surface texture: Areal, Part 2: Terms, definitions and surface texture parameters

Lee DH, Lee SJ, Choi S (2011) A study on 3D roughness analysis of rock joints based on surface angularity. Tunn Under Space Technol 21:494–507

Li YR, Huang RQ (2015) Relationship between joint roughness coefficient and fractal dimension of rock fracture surfaces. Int J Rock Mech Min Sci 75:15–22

Li YR, Zhang YB (2015) Quantitative estimation of rock joint roughness coefficient using statistical parameters. Int J Rock Mech Min Sci 77:27–35

Li YR, Xu Q, Aydin A (2016) Uncertainties in estimating the roughness coefficient of rock fracture surfaces. Bull Eng Geol Environ:1–13

Liu XG, Zhu WC, Yu QL, Chen SJ, Li RF (2017) Estimation of the joint roughness coefficient of rock joints by consideration of two-order asperity and its application in double-joint shear tests. Eng Geol 220:243–255

Marlinverno AA (1990) A simple methods to estimate the fractal dimension of a self affine series. Geophys Res Lett 17(11):1953–1956

Tang ZC, Xia CC, Song YL (2012) Discussion about Grasselli's peak shear strength criterion for rock joints. Chin J Rock Mech Eng 31(2):356–364

Tatone BSA (2009) Quantitative Characterization of Natural Rock Discontinuity Roughness In-situ and in the Laboratory. Master thesis. University of Toronto

Tatone BSA, Grasselli G (2010) A new 2D discontinuity roughness parameter and its correlation with JRC. Int J Rock Mech Min Sci Geomech 47:1391–1400

Tse R, Cruden DM (1979) Estimating joint roughness coefficients. Int J Rock Mech Min Sci Geomech Abstr 16:303–307

Wakabayashi N, Fukushige I (1992) Experimental study on the relation between fractal dimension and shear strength. In: Proceedings of the international symposium for fractured and joint rock masses. Berkeley: California; p.101–110

Yang ZY, Lo SC, Di CC (2001) Reassessing the joint roughness coefficient (JRC) estimation using Z2. Rock Mech Rock Eng 34:243–251

Yu XB, Vayssade B (1991) Joint profiles and their roughness parameters. Int J Rock Mech Min Sci Geomech Abstr 28:333–336

Zhang P, Li N, Chen XM (2009) A new representation method for three-dimensional surface roughness of rock fracture. Chin J Rock Mech Eng 28(9):3478–3483

Zhang GC, Karakus M, Tang HM, Ge YF, Zhang L (2014) A new method estimating the 2D joint roughness coefficient for discontinuity surfaces in rock masses. Int J Rock Mech Min Sci 72:191–198

Zheng B, Qi S (2016) A new index to describe joint roughness coefficient (JRC) under cyclic shear. Eng Geol 212:72–85